On the Electronic Spectrum of Actinomycin D

Julia C. Tai, William S. Craig, and Bruce P. Gaber*

Contribution from the Department of Natural Sciences, University of Michigan-Dearborn, Dearborn, Michigan 48128, and the Department of Chemistry, University of Oregon, Eugene, Oregon 97403. *Received May 17, 1976*

Abstract: The phenoxazone chromophore of actinomycin D has been subjected to a variable electronegativity self-consistent field calculation with configuration interaction (VESCF-CI) and the theoretical calculation compared with experimental data. Spectral bands at 441 and 429 nm arise from $\pi \rightarrow \pi^*$ transitions largely localized on the quinoidal portion of the chromophore. A third band near 395 nm is thought to be an $n \rightarrow \pi^*$ transition but is not included in the calculation. Only bands below 248 nm contain substantial contributions from the phenyl moiety of the phenoxazone ring. Oscillator strengths and transition moment directions have been calculated. Computation is simplified, with little loss of precision, by excluding the two carbonyl groups from the calculation.

Although the electronic spectrum of the antitumor drug actinomycin D has been extensively exploited for studies of drug-nucleotide interactions,[1-11] the origin of the transitions involved has never been investigated. Consequently, the analysis of spectroscopic data for actinomycin D has been complicated and uncertain. Reported here are the results of a preliminary molecular orbital treatment of the phenoxazone chromophore of actinomycin D using a variable electronegativity self-consistent field calculation with configuration interaction (VESCF-CI). The calculation provides a set of transition energies and an estimate of the contribution of individual atomic orbitals to each transition. We have compared our theoretically derived transition energies with experimental data, thereby assigning the major bands of the absorption spectrum.

Experimental Section

Materials and Equipment. Actinomycin D was obtained from P-L Laboratories and used without further purification. Spectra were taken of samples freshly prepared in either water or ethanol at a concentration of 2.72×10^{-5} M.

Reduction with $NaBH_4$ was accomplished by adding a minimal amount of the reagent to a cuvette containing a solution of actinomycin D. The solution was instantly decolorized. Similar results were obtained with sodium cyanoborohydride. Simply increasing the pH of an actinomycin D solution to pH 11 did not cause any significant loss of color.

Spectra were recorded on a Cary 118C UV-visible spectrophotometer operated in either direct absorbance or first derivative mode.

Computation Procedure. The atoms in the chromophore of the actinomycin D molecule are numbered as in Figure 1. (The same numbering system is used to designate individual atomic orbitals in Table II.) A modified VESCF-CI treatment which takes into account the effects of substituents on the charges of the atoms carrying the π orbitals was used. All singly excited states were included in the CI matrix. This gave a total of 100 configurations when all 20 atomic orbitals were included in the calculation. The method as well as the parameters for carbon atoms were described earlier.[12] The parameters used for orbitals 11, 18, and 20 were those of carbonyl oxygen[13] and for orbitals 7 and 10 those of pyridine and furan, respectively.[14] It was recognized that these parameters should perhaps be modified to better describe the particular molecule on hand. However, since our primary interest was to identify the nature of the electronic transitions, we did not think adjustment of parameters was of major concern at this time.

The geometry of the chromophore was taken from Sobell and Jain.[15] The three rings lie very nearly on the same plane, with one of the two carbonyl oxygen atoms pointing above and the other below the plane. Calculations which included all of the 20 orbitals showed that these two carbonyl groups mixed very little with the rest of the chromophore or with each other. We next did a calculation including orbitals 1-16 only. Comparison of the results from the two calculations showed that corresponding transitions agreed very well both in transition energies and in transition moments. The maximum difference in transition energy is 0.04 eV and in transition moment 10%. We therefore omitted the two carbonyl groups in subsequent calculations. It is perhaps important to note that the cpu time for the 16-orbital treatment was only one-third of that for the 20-orbital treatment which took about 180 s.

* Address inquiries to this author at the University of Oregon.

Results

The electronic spectrum of actinomycin D (Figure 2) is characterized by an intense, asymmetric, visible absorption band centered at 441 nm. The first derivative of the absorption spectrum suggests that the visible band consists of two components. This structure is clearly evident in the spectrum recorded in ethanol (Figure 3) in which major features are seen at 446 and 418 nm as well as a very weak derivative inflection near 380 nm. In the ultraviolet principal bands occur at about 200 and 240 nm, with shoulders near 275 and 295 nm.

The results of the calculation are shown in Table I together with the experimental data determined from the spectrum in Figure 1. The notation used in Table I to describe the transitions is interpreted in the following way: V_0 represents the ground state configuration (molecular orbitals 1-9 are the bonding π orbitals); V_{ij} denotes the configuration in which an electron in the ith molecular orbital has been excited to the jth molecular orbital. Thus "$V_0 \rightarrow V_{9,11}$" means a $\pi \rightarrow \pi^*$ transition with V_0 the π ground state and the π^* excited state one in which a single electron from MO 9 has been promoted to an antibonding orbital, MO 11. The constituent *atomic orbitals* from which the molecular orbitals derive are indicated in Table II which presents the percent contribution of atomic orbitals to molecular orbitals 6-13. These are the MO's involved in transitions that are included in Table I. The numerical designation for atomic orbitals in Table II corresponds to Figure 2. For example, molecular orbital 8 is a combination consisting of 34% contribution from the amino nitrogen (atomic orbital 12) and greater than 10% each from quinoidal ring carbon (AO 4) and the bridge oxygen (AO 10).

The directions of the transition moments were also calculated. If we let the x-y plane be determined by atoms 6, 7, and 10, with the latter two atoms on the y axis, the transition moments were found to lie approximately in the x-y plane. The angles between the $+x$ axis and the transition moment are listed in Table I. Note that moments for the 441 and 429 nm bands lie on the long axis of the chromophore.

Discussion

There is generally good agreement between the calculated and observed transition energies. This is particularly so for the

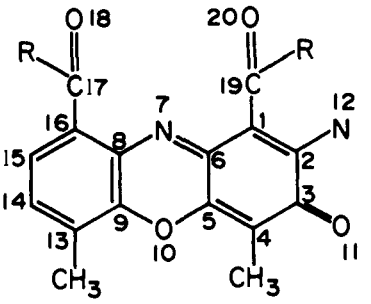

Figure 1. The phenoxazone chromophore of actinomycin D. R is a cyclic pentapeptide moiety.

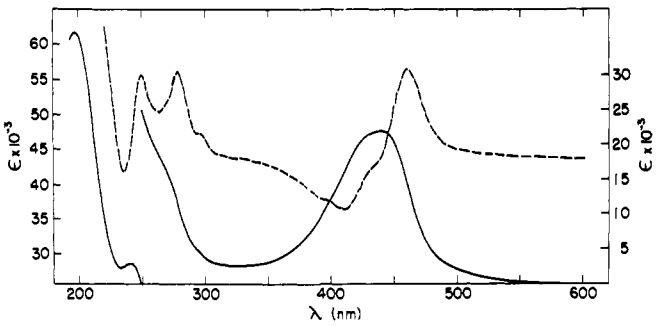

Figure 2. Electronic spectrum of actinomycin D in water (solid line). The scale on the left ordinate refers to the portion of the absorption spectrum below 250 nm. The first derivative of the absorption spectrum is denoted by the dashed line. The intensity of the derivative spectrum is in arbitrary units. The first derivative spectrum is useful for visualization of weak spectral feature. Note, for example, the resolution of the broad band at 440 into two inflections in the derivative curve.

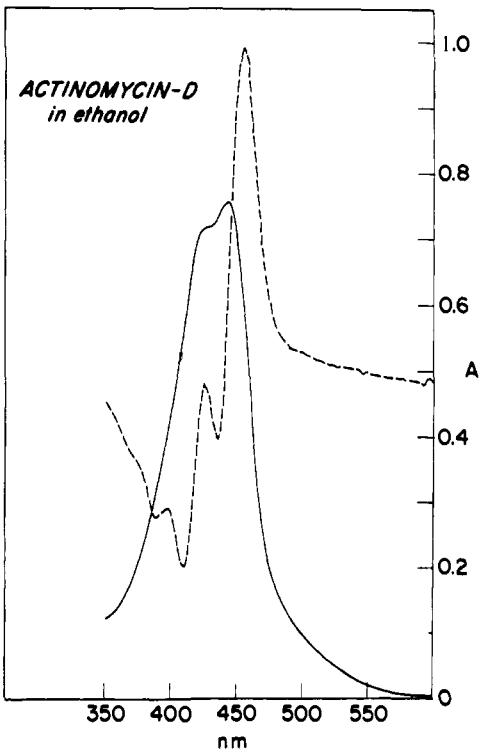

Figure 3. Electronic spectrum of actinomycin D in ethanol (solid line). The first derivative of the absorption spectrum is shown by a dashed line.

prominent bands observed at 441 (calcd 452 nm), 272 (calcd 286 nm), 240 (calcd 248 nm), and 199 nm (calcd 203 nm). These bands are, therefore, properly characterized as $\pi \rightarrow \pi^*$ transitions. Of course, these data must be viewed with the *caveat* that only a calculation over the π skeleton has been attempted. Therefore, although the agreement with experiment is quite good the calculation, in some instances, permits only a speculative rather than an absolute interpretation. For example, some difficulty is encountered in assigning the $V_0 \rightarrow V_{8,10}$ transition. As can be seen in Table I, there are two bands which are observed close to the calculated value of 402 nm, either of which may be assigned to that transition. The two bands, one at 429 nm and the other at 395 nm, appear as shoulders in aqueous spectra and as more distinct transitions in ethanol. Without further information, we can only say that one of these is perhaps an $n \rightarrow \pi^*$ transition which is not included in our calculation.

Similarly, interpretation of the complicated UV region must be approached with some caution. However, the discrepancies between the calculated and observed transitions at 199 and 229 nm are thought to be due to the fact that oscillator strength is a highly sensitive function of molecular orbitals, and usually a factor of 2 to 3 is tolerated in the calculation. We therefore feel that the absorption at 228 nm is much weaker than calculated and is obscured by a large amount of band overlap and

Table I. Calculated and Experimental Transition Energies and Oscillator Strengths

	Wavelength, nm (transition energy, eV)		Oscillator strength[c]		Transition moment,[d] deg
Transition[a]	Calcd	Obsd[b]	Calcd	Obsd	Calcd
$V_0 \rightarrow V_{9,10}$	452 (2.75)	441 (2.81)	0.44	0.44	0
$V_0 \rightarrow V_{8,10}$	402 (3.09)	429 sh (2.89)	0.49	0.43	0
		395 sh (3.14)		0.21	
$V_0 \rightarrow V_{7,10}$	305 (4.07)		0.02		180
$V_0 \rightarrow V_{9,11}$	286 (4.34)	272 sh (4.56)	0.14	0.31	−50
$V_0 \rightarrow V_{6,10}$	276 (4.49)		0.05		0
$V_0 \rightarrow V_{8,11}$	248 (5.00)	240 (5.17)	0.89	0.58	180
$V_0 \rightarrow V_{9,13}$	241 (5.14)		0.03		0
	234 (5.30)		0.06		−90
	228 (5.43)		0.31		180
$V_0 \rightarrow V_{8,13}$	203 (6.12)	199 (6.23)	0.23	>1	−20

[a] The notations under this column represent the most important configuration of the states. The notation V_0 represents the ground state configuration and V_{ij} the configuration in which an electron in the ith molecular orbital has been promoted to the jth molecular orbital. Those transitions that lack notation are, as a result of extensive configuration interaction, a mixture of many equally important transition types. [b] Taken from the data in Figure 1. [c] Oscillator strengths (f) were calculated from the extinction coefficients (ϵ) using the formula $\epsilon = 49\,773f$ to fit the calculated value for the longest wavelength transition. The extinction coefficients were calculated from our own spectra based on a previously obtained value of 21 900 for the observed transition at 441 nm.[6] [d] Direction of the transition moment expressed as angles measured clockwise from the $+x$ axis. See text for details.

Table II. Contributions from Atomic Orbitals (AO's) to Molecular Orbitals (MO's)

Molecular orbital[a]	AO's contributing more than 25%	AO's contributing more than 10%	AO's contributing more than 1%
6		4, 5, 9, 14, 15	3, 7, 13
7	13, 16		1, 3, 4, 5, 11
8	12 (33.5%)	4, 10	2, 3, 7, 13, 16
9	12 (44.2%)	7	3, 5, 13, 15
10		2, 6, 7, 11	8, 13, 15
11		3, 5, 8, 9, 15	1, 7, 10, 12, 16
12	13, 16	9, 15	1, 2, 4, 7, 12
13	1	2, 4, 8, 14	3, 7, 10, 11, 16

[a] Molecular orbitals are numbered in the order of increasing energy. MO's 1–9 are bonding orbitals.

that the absorption at 199 nm has contributions to its intensity from absorptions at still lower wavelengths.

As a test of our computational method, we have calculated the visible spectrum of 7-NH_2-actinomycin, a derivative which exhibits a visible spectrum red shifted by 65 nm.[16] A red shift of ~10 nm in the longest wavelength transition is calculated along with a substantial (50%) increase in transition moment. Thus the calculation correctly predicts the qualitative features of the 7-NH_2-actinomycin spectrum. Although the calculated shift is small relative to the experimental shift (and suggests the limitations of the calculations), note that in this spectral range 70 nm corresponds to an energy difference of only about 0.4 eV, about the same magnitude as solvent shifts. Further our calculation did not correct for the effect of the σ core polarization on the effective nuclear charge of the atomic orbitals used. Since this correction would be different for the actinomycin molecule itself and for the NH_2 derivative, such a discrepancy between calculated and experimental data is not surprising.

As is evident from Table II, most of the MO's are quite delocalized, as expected, with half or more of the atomic orbitals contributing between 1 and 10%. Molecular orbitals 8 and 9 are the only ones where one atomic orbital contributes more than one-third. The two longest wavelength transitions are therefore similar in that they represent heavy donation of electrons on atom 12 (the amino nitrogen) to other parts of the molecule. It should be noted that with the exception of MO's 7 and 12 the MO's have relatively little contributions from the phenyl portion of the molecule, namely atoms 13–16. Each of the MO's 8, 9, and 10 has only about 8% phenyl ring character, and each of the MO's 6, 11, and 13 has about 20%. We should therefore expect that the first two transitions would not be affected very much by the phenyl ring. Indeed, we did a calculation not including atoms 13–16 and found the transition energies to differ by less than 0.1 eV although the oscillator strengths changed considerably. Furthermore, as would be expected, with the phenyl ring omitted from the calculation there was no calculated transition corresponding to $V_0 \rightarrow V_{7,10}$. Thus, the two longest wavelength $\pi \rightarrow \pi^*$ transitions result almost solely from the quinoidal portion of the phenoxazone ring system. Chemical confirmation of this observation is given in that, upon reduction of the quinoidal portion with sodium borohydride, all the absorption bands in the visible region disappear, while the ultraviolet structure remains intact.

Our calculations establish the important conclusion that the visible absorption of actinomycin D derives almost entirely from the quinoidal ring. Thus, the hypo- and bathochromic shifts resulting from complexation of actinomycin D by nucleotides may be explained as a perturbation of the quinoidal π system alone; an observation which agrees with and tends to confirm the experiments of Krugh and Neely.[17] As we have shown, eliminating the benzoid ring entirely from the calculation results in only a small change in the parameters of the visible transitions. It is reasonable to suppose that a base stacking interaction with the benzoid ring would not manifest as significant perturbation of the visible bands. For example, the exciton interaction for an ApA dimer is 740 cm^{-1} at 260 nm,[18] while the separation between the principal UV and visible bands of actinomycin D is 19,000 cm^{-1}. This large energy gap would also seem to preclude direct base–quinoid ring interaction. More likely, therefore, the bathochromic and hypochromic shifts result from environmental effects (e.g., solvation). Whatever their origin, we suggest that these spectral changes report only *interactions with the quinoidal portion of the chromophore.* This concept provides a means of testing the hypothesis that the rings (benzoid and quinoid) exhibit individual selectivity in their nucleotide binding.[19]

Note Added in Proof. It has been pointed out to us by Professor Crothers that the presence of a strong optically active band near 375 nm[20] suggests that the weak 395 nm feature may be an $n \rightarrow \pi^*$ transition.

Acknowledgment. Our thanks to Dr. Robert W. Wilson for valuable discussions. This work was supported in part by grants from the Research Corporation; Institutional Grant IN-40 to the University of Michigan from the American Cancer Society; Campus Grants Committee, the University of Michigan–Dearborn.

References and Notes

(1) W. Kersten, *Biochim. Biophys. Acta*, **47**, 610 (1961).
(2) M. Gellert, C. E. Smith, D. Neville, and G. Felsenfeld, *J. Mol. Biol.*, **11**, 445 (1965).
(3) R. Müller and D. M. Crothers, *J. Mol. Biol.*, **35**, 251 (1968).
(4) D. M. Crothers, S. L. Sabol, D. I. Ratner, and W. Müller, *Biochemistry*, **7**, 8817 (1968).
(5) D. M. Crothers and D. I. Ratner, *Biochemistry*, **7**, 1823 (1968).
(6) H. Ziffer, K. Yamaoka, and A. Mauger, *Biochemistry*, **7**, 996 (1968).
(7) R. B. Homer, *Arch. Biochem. Biophys.*, **129**, 405 (1969).
(8) R. D. Wells and J. E. Larson, *J. Mol. Biol.*, **49**, 319 (1970).
(9) R. Schara and W. Muller, *Eur. J. Biochem.*, **29**, 210 (1972).
(10) T. R. Krugh, *Proc. Natl. Acad. Sci. U.S.A.*, **69**, 1911 (1972).
(11) R. Bittman and L. Blau, *Biochemistry*, **14**, 2138 (1975).
(12) N. L. Allinger, J. C. Tai, and T. W. Stuart, *Theor. Chim. Acta*, **8**, 101 (1967).
(13) N. L. Allinger, T. W. Stuart, and J. C. Tai, *J. Am. Chem. Soc.*, **90**, 2809 (1968).
(14) J. C. Tai and N. L. Allinger, *Theor. Chim. Acta*, **15**, 133 (1969).
(15) H. M. Sobell and S. C. Jain, *J. Mol. Biol.*, **68**, 21 (1972).
(16) E. J. Modest and S. K. Sengupta, *Cancer Chemother. Rep., Part 1*, **58**, 35 (1974).
(17) T. R. Krugh and J. W. Neely, *Biochemistry*, **12**, 1775 (1973).
(18) M. Gueron, J. Eisinger, and A. A. Lamola, "Basic Principles in Nucleic Acid Chemistry", P. O. P. Ts'O, Ed., Vol. 1, Academic Press, New York, N.Y., 1974, pp 331.
(19) T. R. Krugh and J. W. Neely, *Biochemistry*, **12**, 4418 (1973).
(20) Y. Courtois, W. Guschlbauer, and P. Fromageot, *Eur. J. Biochem.*, **6**, 106 (1968).